Pergamon

Tetrahedron 57 (2001) 8357–8367

TETRAHEDRON

Research on anti-HIV-1 agents. Part 2: Solid-phase synthesis, biological evaluation and molecular modeling studies of 2,5,6-trisubstituted-4(3*H*)-pyrimidinones targeting HIV-1 reverse transcriptase☆

Maurizio Botta,[a,*] Federico Corelli,[a,*] Giovanni Maga,[b] Fabrizio Manetti,[a] Michela Renzulli[a] and Silvio Spadari[b]

[a]*Dipartimento Farmaco Chimico Tecnologico, Università degli Studi di Siena, Via Aldo Moro, I-53100 Siena, Italy*
[b]*Istituto di Genetica Biochimica ed Evoluzionistica del CNR, Via Abbiategrasso 207, I-27100 Pavia, Italy*

Received 26 March 2001; revised 9 July 2001; accepted 2 August 2001

Abstract—A small library of 2,6-disubstituted- and 2,5,6-trisubstituted-4(3*H*)-pyrimidinones has been synthesized by solid-phase synthesis starting from a modified Merrifield resin. The new pyrimidinones have been tested in vitro for their ability to inhibit HIV-1 RT in comparison with nevirapine. Interestingly, some of them showed moderate activity against recombinant RTs carrying mutations conferring resistance to TIBO/nevirapine. The possible mode of binding between Y188L mutant of RT and the new compounds has been studied through a molecular modeling approach. © 2001 Elsevier Science Ltd. All rights reserved.

1. Introduction

Due to the enormous progress made in genomic sciences and molecular biology, an ever-growing number of new biological targets of pharmacological interest is emerging. To meet the increasing demand for novel and diverse small molecular-weight compounds necessary for screening, combinatorial or parallel chemistry are currently the focus for the creation of novel and diverse compound collections.[2] Solid-phase synthesis (SPS) is playing a decisive role in the ongoing development of combinatorial chemistry, mainly because it offers striking advantages in terms of synthetic flexibility, such as: (i) the ease of chemistry; (ii) the possibility of using high concentrations of reagents to drive reactions to completion; (iii) the elimination of purification steps *en route*, since impurities and excess reagents can be removed by simple washing of the solid phase; (iv) the straightforward nature of parallel SPS; (v) the possibility of automation.[3]

As a part of a project devoted to the development of efficient methodologies for a parallel version of the combinatorial synthesis of novel antivirals on solid support, we have focused our attention on pyrimidine derivatives, due to the broad range of useful properties they display,[4] among with the antiviral and anticancer activities of some of these derivatives (as well as of their corresponding nucleosides) which have great biological significance. In particular, in the last few years, some uracil and pyrimidinone derivatives substituted at the C-5 and C-6 positions have emerged in the field of antiviral chemotherapy.[5–7] Among the biologically relevant 6-substituted uracils, HEPT (Fig. 1) and analogues thereof have been chosen as candidates for clinical trials,[8]

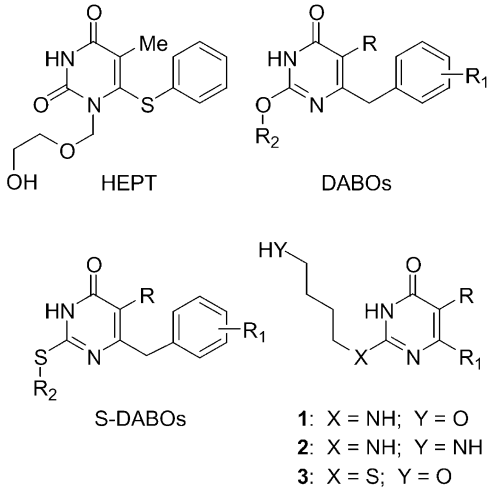

Figure 1.

☆ See Ref. 1.

Keywords: solid-phase synthesis; pyrimidinones; anti-HIV-1 agents; molecular docking.

* Corresponding authors. Tel.: +39-0577-234306; fax: +39-0577-234333. Tel.: +39-0577-234308; fax: +39-0577-234333; e-mail: botta@unisi.it; corelli@unisi.it

PII: S0040-4020(01)00815-8

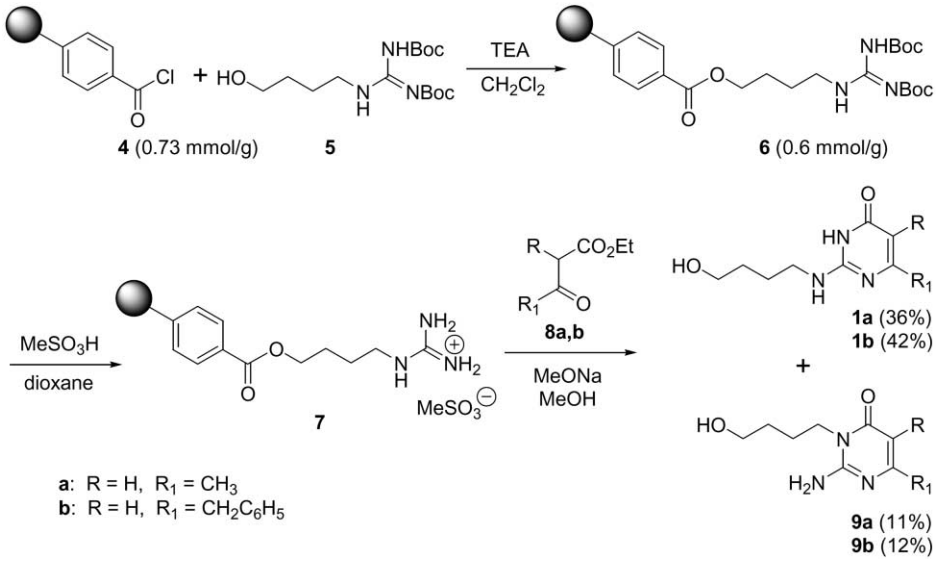

Scheme 1.

and, more recently, 2,6-disubstituted and 2,5,6-trisubstituted-4(3*H*)-pyrimidinones (DABOs and S-DABOs)[9] have shown very good potential as antiviral agents inhibiting HIV-1 reverse transcriptase (RT).[10]

During the course of our studies on anti-HIV-1 agents[11] we became interested in developing an SPS methodology for 2,5,6-trisubstituted-4(3*H*)-pyrimidinones of general structure **1**–**3** which would allow the maximization of the number and chemical diversity of these compounds. In this report we describe in full the synthesis of **1a**, **b**[12] as well as of the new compounds **2b**, **c** and **3a**–**c** through different SPS approaches. The new pyrimidinone derivatives were tested against a panel of recombinant HIV-1 RTs from both wild type (wt) and mutant viruses and their possible binding mode to the non-nucleoside inhibitors binding site of the viral enzyme was studied by means of molecular mechanics calculations.

2. Results and discussion

2.1. Chemistry

6-Substituted isocytosine derivatives can be prepared following two different approaches: (i) by reaction of 2-methoxy- or 2-methylthiopyrimidinones with an excess of amide anions in refluxing tetraline, or (ii) by condensing guanidines with β-keto esters.[13] The first approach suffers from some drawbacks, as the experimental conditions required make the use of aminoalcohols problematic and sometimes cause the nucleophilic substitution to occur at the 4 position of the ring,[14] while the second method seemed to be more appropriate in our case. Considering that a *N*-(4-hydroxybutyl)guanidine moiety would be a common feature of the target compounds **1**, a convergent and versatile strategy called for immobilizing this group first, and then subjecting it to condensation with different β-keto esters to prepare diverse sets of potential RT inhibitors. Since the presence of a free hydroxyl is not compatible with the conditions of the condensation reaction, we decided to employ *O*-immobilized *N*-4-(hydroxybutyl)guanidine, wherein the linker group, besides being a cleavable site of attachment for the molecule to a solid support, also serves as an oxygen protecting group.

The next issue to be addressed was the choice of a polymeric support that would be available in insoluble bead form for easy separation, mechanically stable to physical manipulations, inert to reaction conditions, hydrophobic and capable of swelling in organic solvents to facilitate reactions. Addressing all of these requirements, the commercially available 2% crosslinked Merrifield peptide resin (1–1.5 mmol Cl g^{-1}) seemed a suitable starting material. However, in order to reproduce as truly as possible the conditions used in solution,[12] we chose as the solid support the modified Merrifield resin **4**[15] (Scheme 1). Thus, **4** was reacted with 3 mol equiv. of N^2,N^3-bis(*tert*-butoxycarbonyl)-N^1-(4-hydroxybutyl)guanidine **5**, obtained in 85% yield starting from commercially available *N*,*N*′-bis(*tert*-butoxycarbonyl)-*S*-methylisothiourea and 4-aminobutanol following a procedure already reported for similar compounds,[16] to give the polymer-bound guanidine **6**, the *O*/*N* selectivity in this acylation reaction being clearly due to the steric hindrance exerted by the bulky Boc groups. The resin **6** was analyzed for residual Cl to determine its loading and this was found to be no more than 0.41 mmol g^{-1}; therefore **4** was again exposed to excess **5** under the same conditions to yield the resin **6** showing a loading of 0.60 mmol g^{-1} (no Cl determined by microanalysis). In consideration of these results, all the following reactions were performed twice and assumed to be quantitative. The overall yield of the solid phase sequence was calculated weighing the cleaved final product after chromatografic purification. Removal of the Boc protecting groups from **6** by the action of methanesulfonic acid (MSA) in refluxing dioxane led to the resin **7**, which was in turn condensed with ethyl 3-oxobutanoate (**8a**) in the presence of sodium methoxide (methanol, reflux, 20 h). Under these conditions, not only condensation to pyrimidinone, but also cleavage of 4-benzoate group occurred, leading to a mixture of fully deprotected 2,6-disubstituted-4(3*H*)-pyrimidinone **1a** and

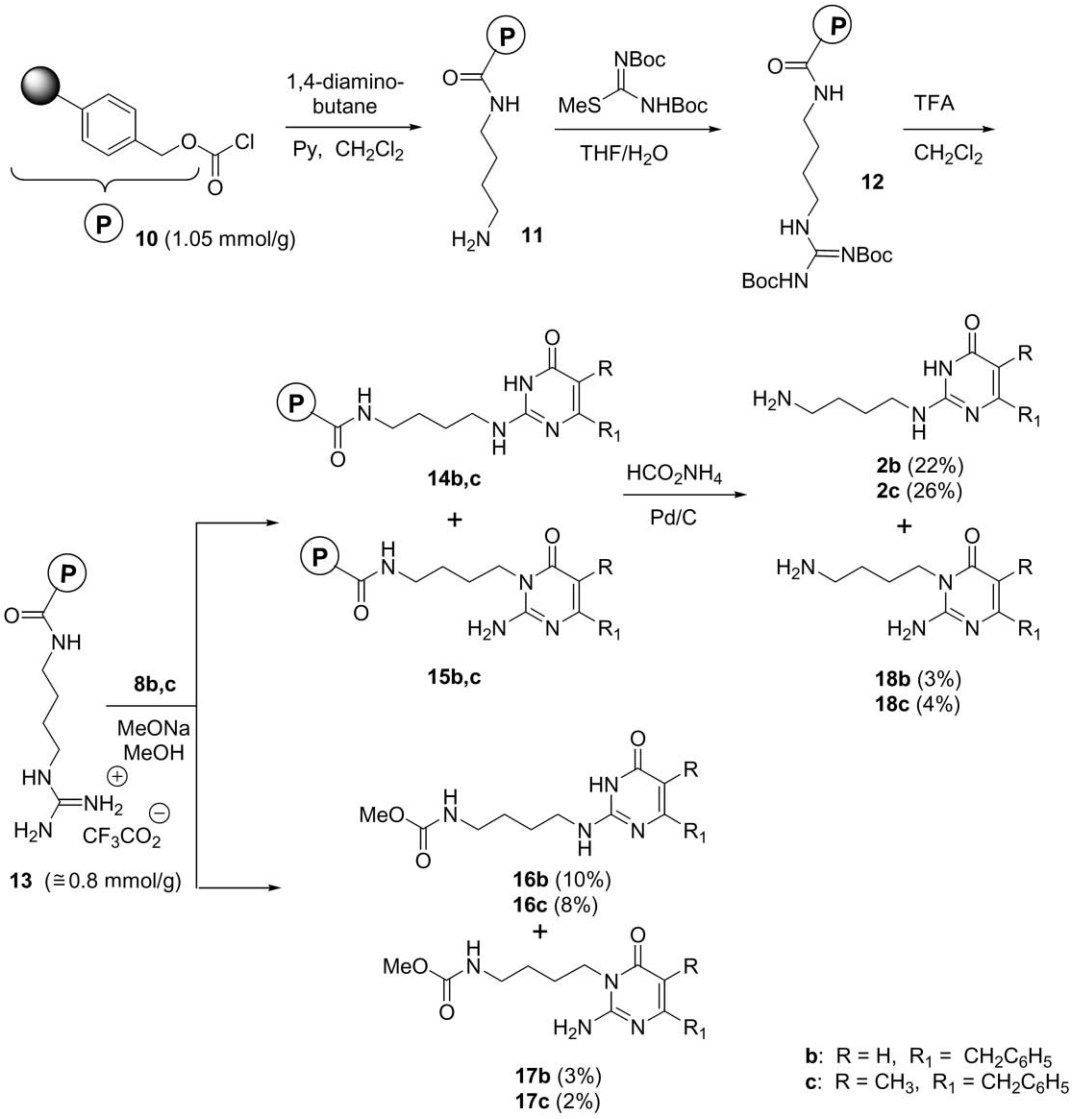

Scheme 2.

2,3,6-trisubstituted-4(3*H*)-pyrimidinone **9a**.[17] Removal of the resin by filtration, followed by chromatographic separation of the filtrate, gave the pure compounds **1a** and **9a** in 36 and 11% yield, respectively, calculated based on the acyl chloride functionality of the modified Merrifield resin. Similarly, reaction of **7** with ethyl 3-oxo-4-phenylbutanoate (**8b**) provided **1b** and **9b** in 42 and 12% yield, respectively.

Structures of compounds **1** and **9** were assigned on the basis of spectroscopic data. In the ^{1}H NMR spectrum of **1**, the signal of 1′-methylene centered at 3.39 ppm is a broad triplet (J=5.9 Hz) due to the coupling with both the vicinal methylene and NH groups. Conversely, the ^{1}H NMR spectrum of compound **9** shows the 1′-methylene resonating at 3.68 ppm as a clean triplet (J=6.4 Hz) as well as a broad signal at 6 ppm that is clearly due to a C-2 primary amino group. These data enabled us to assign the 3-alkylated structure to compounds **9**.

This first SPS approach to the target pyrimidinones was unsatisfactory in that it suffered from two main drawbacks: (i) the yields of the reaction sequence necessary to prepare the modified Merrifield resin **4** proved to be rather erratic in our hands; (ii) the tethering strategy is not appropriate for compounds like **2**, since the amide bond requires very harsh conditions to be cleaved. Accordingly, we next undertook a more generalized approach based on the exploitation of the modified resin **10** (Scheme 2), that would allow for the easy anchoring of alcohol or amine functionalities as benzylic carbonates or carbamates as well as their fast release via protonolysis or hydrogenolysis, respectively.

Treatment of resin **10**[18] (Scheme 2) with excess 1,4-diaminobutane (pyridine, CH_2Cl_2) afforded the polymer-bound carbamate **11**, which was then converted into the Boc-protected guanidine **12** by guanylation with *N*,*N*′-bis(*tert*-butoxycarbonyl)-*S*-methylisothiourea. Selective removal of the Boc groups (no cleavage of the benzyl carbamate function was observed) was accomplished by using a 25% solution of trifluoroacetic acid in dichloromethane at 0°C for 3 h, thus leading to the guanidine salt **13**,[19] which in turn was cyclized to the expected polymer-bound aminopyrimidinones **14b**, **c** and **15b**, **c** by condensation with β-keto esters **8b**, **c** in the presence of sodium

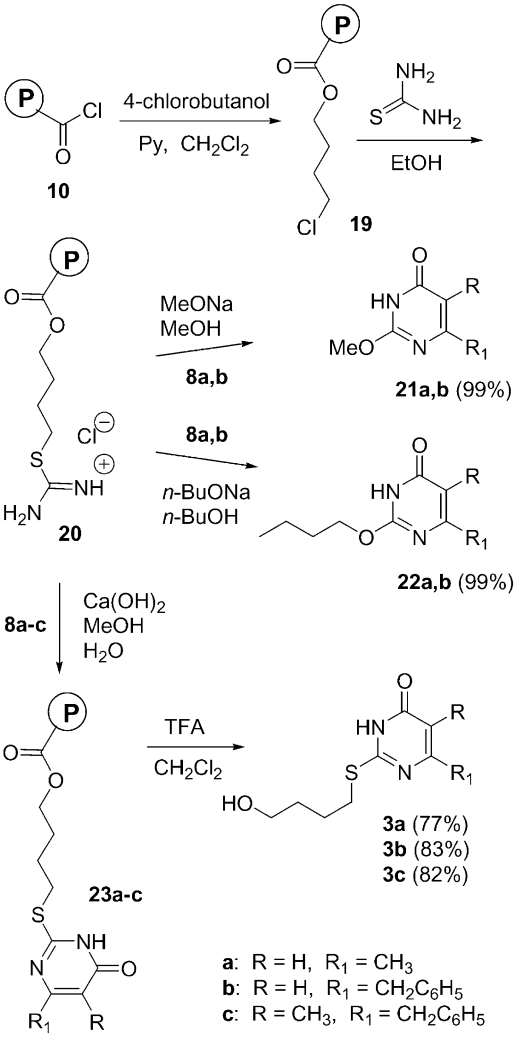

Scheme 3.

methoxide as a base. Actually, the carbamate linkage resulted to be not completely unaffected by the basic conditions adopted in this reaction, as small amounts of compounds **16** and **17** were released in solution, although in very low yield (10 and 3%, respectively). Catalytic transfer hydrogenation with ammonium formate and Pd/C in refluxing methanol efficiently cleaved the benzyl carbamate linkage of **14** and **15** to yield a mixture of **2b**, **c** and **18b**, **c**, which were separated by preparative TLC to give the pure compounds **2** (22–26% yield) and **18** (3–4% yield).

Table 1. In vitro inhibitory activity of selected compounds against recombinant HIV-1 reverse transcriptase

	K_i (μM)						
HIV-1 RT	**1b**	**2b**	**2c**	**3b**	**3c**	**21c**	Nevirapine
Wild type	410	70	97	100	70	23	0.4
L100I	525	95	n.a.[a]	200	73	70	9
K103N	840	n.a.	n.a.	n.a.	83	n.a.	7
V106A	75	n.a.	n.a.	157	96	n.a.	10.5
V179D	n.a.	n.a.	98	139	115	n.a.	0.35
Y181I	n.a.	n.a.	n.a.	516	578	n.a.	9
Y188L	n.a.	n.a.	n.a.	207	58	n.a.	0.35

[a] n.a.=not active (K_i>1 mM).

The condensation of **13** with β-keto esters exhibited in this case a higher degree of regioselectivity with respect to the analogous reaction described for **7**, as the ratio between **2** and **18** was never less than 6.

Having secured an easy access to compounds **2**, we went on investigating the possibility to get isosteres **3** through a similar SPS approach. Accordingly, resin **10** (Scheme 3) was treated with excess 4-chlorobutanol to give the polymer-bound carbonate **19**, which was then converted into the isothiouronium salt **20** by reaction with thiourea in refluxing ethanol. When **20** was condensed with ethyl 3-oxobutanoate (**8a**) under the usual conditions (0.13 M sodium methoxide in methanol), 2-methoxy-6-methyl-4(3*H*)-pyrimidinone (**21a**) was obtained in quantitative yield after filtration of the resin and chromatographic purification of the filtrate. This product clearly arises from nucleophilic displacement of a thiolate anion by sodium methoxide, but in the light of the harsh conditions necessary to perform this reaction on preformed 2-methylthio-4(3*H*)-pyrimidinones, this displacement most likely occurs on isothiouronium salt **20** leading to the release of *O*-methylisourea that subsequently reacts with **8a** *in solution* to afford **21a**. This sequence proved to also work well when a different β-keto ester (such as **8b**) and/or a different alkoxide (*n*-BuONa in *n*-BuOH) were employed, thus allowing the preparation in moderate to excellent yield of other compounds (**21b** and **22a**, **b**) belonging to the DABO family of anti-HIV-1 RT inhibitors. This approach to the synthesis of DABO derivatives compares quite favourably with the solution-phase procedure previously described,[21] since it does not require the preliminary preparation of different *O*-alkylisoureas, not always readily accessible, nor the transformation under vigorous nucleophilic conditions of pyrimidinone scaffolds, and provides less complex reaction mixtures from which the final products can be more easily isolated in a pure form.

In order to obtain our target compounds **3**, less nucleophilic conditions had to be adopted in the condensation reaction between the polymer-bound isothiouronium salt **20** and β-keto esters **8**. Thus, the use of $Ca(OH)_2$ as a base in a 1:1 mixture of methanol and water at room temperature for 72 h proved to be quite an efficient system in promoting the condensation reaction to thiopyrimidinones **23a–c** while preventing any detachment of product from the solid support. Finally, compounds **3a–c** were obtained in 77–83% yield under very mild conditions through the CF_3CO_2H-mediated cleavage of the carbonate functionality of **23a–c**.

In conclusion, the SPS methodologies reported here allow the synthesis of diverse families of compounds in an easy and profitable way, showing good potential in the preparation of combinatorial libraries of 4(3*H*)-pyrimidinones bearing different alkyl substituents at the 5 and/or 6 position and various functionalities at 4′ and 1′ position on the C-2 side chain.

2.2. Biological assays

Compounds **1b**, **2b**, **2c**, **3b**, **3c,** and **16c** were evaluated in enzyme assays against recombinant HIV-1 RTs from both

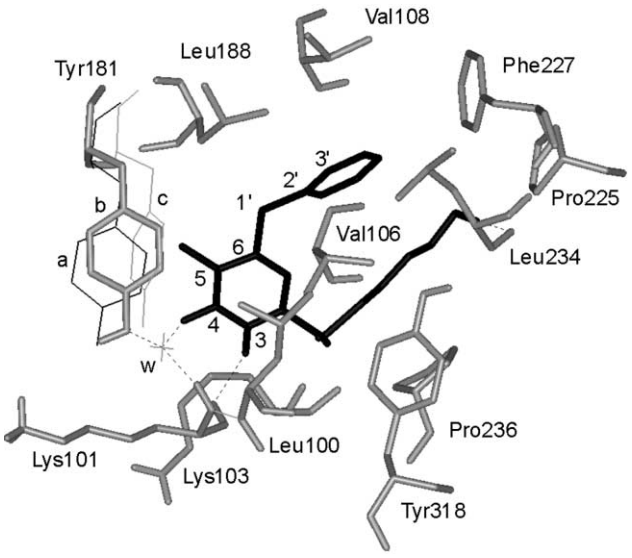

Figure 2. Compound **3c** (black thick lines) docked into the NNRTI binding site of the Y188L mutated RT. For safe of clarity, only the amino acids surrounding the inhibitor have been reported (grey thick lines) and labelled. W is a water molecule included in the calculations. Three hydrogen bonds between the carbonyl at the position 4 and the water molecule, the NH group at position 3 and Lys101, and the hydroxy group at the end of the C-2 side chain and Leu234, respectively, have been found (dashed black lines). The complexes **3c**– and HEPT–RT (coded 1rti[25] in the Brookhaven protein data bank) were, in turn, compared with the structure of the unliganded enzyme (1rtj[28] in the Brookhaven protein data bank) by superposition, at the backbone level, of the amino acid sequences 94–118, 156–215, 225–243, 317–319, and 137–139, according to a previous comparison of the NNRTI binding sites of both the unbound and the inhibited RT enzyme.[22] As a consequence of these superpositions, the Tyr181 side chain has been shown in the figure in three different conformations: (a) (black thin lines), orientation in the unbound RT; (b) (grey thick lines), Tyr181 side chain in the complex with **3c**; and, finally, (c) (grey thin lines), in the complex with HEPT. Dihedral angles C5–C6–C1′–C2′ (155°) and C6–C1′–C2′–C3′ (142°) define the spatial relationship between both the pyrimidine and the phenyl rings of the inhibitor.

wild tipe (wt) and clinically relevant mutant viruses resistant to TIBO/nevirapine (L100I, K103N, V106A, Y181I, and Y188L) or pyridinone derivatives (V179D), using nevirapine as reference drug. The ability of these compounds to inhibit the recombinant enzymes is reported in Table 1 as K_i (μM) values. In general, all the tested compounds (with the only exception of **16c**) exhibit K_i values too high to be considered of interest as drug candidates against wt recombinant RT. However, their spectrum of activity against mutant enzymes deserves some comments. Thus, the activity of **3c** against all but Y181I of the recombinant RTs as well as the inhibiting activity displayed by **1b** against V106A rRT, the activity of **2b** and **21c** against both wt and L100I enzymes and the ability of **2c** to inhibit wt and V179D rRTs suggest that these compounds can actually bind to RTs. Moreover, the activity profile of the tested compounds is in agreement with the results of previous structure–activity relationship studies on HEPT[22] and S-DABO[9b,23] derivatives, that have clearly highlighted the crucial role played by the substituent at position 5 of the pyrimidine ring in binding to RT. In fact, the introduction of a 5-methyl group on the heterocyclic ring led to a significant enhancement of the inhibiting activity against rRTs, as evidenced by the comparison of the anti-enzymatic properties of **3b** and the corresponding 5-methyl derivative **3c**. In conclusion, compounds of general structure **1**, **2**, and **3** may represent interesting leads for further structural optimization in the search for novel RT inhibitors.

2.3. Molecular modeling studies

In crystal structures of unliganded HIV-1 RT, the non-nucleoside inhibitor binding site (NNIBS) does not exist. During the process of inhibitor binding, significant conformational changes occur in the orientation of the side chains of some residues (particularly Tyr181 and Tyr188),[24] leading to the formation of the hydrophobic pocket accommodating the inhibitor. It is evident from a comparison of the various RT structures that the NNIBS has a very flexible structure, and this flexibility apparently allows the enzyme to accommodate structurally diverse inhibitors having different shapes and sizes. In fact, side chain residues adapt themselves to each bound inhibitor in a highly specific manner, closing about the surface of the drug to make tight van der Waals contacts. These considerations emphasize the opportunity, when a new ligand has to be modeled within the NNIBS, to choose as the input geometry the crystallographic data of the complex between RT and an inhibitor as similar as possible to the compound under study. Accordingly, we chose the RT-HEPT complex[25] as the initial RT model for calculations.

It is well known that many mutations occur at residues which are in direct contact with the inhibitor, several conferring resistance to a range of NNRTIs. Most of these mutations involve a reduction in the size of a hydrophobic side chain leading to a loss of specificity of interaction with the NNRTIs. An example of this general trend is the substitution Y188L (or Y188C or Y188H) that confers resistance to most NNRTIs, presumably by destroying the interaction of the tyrosine ring with the NNRTI rings.

In our case, compound **3c** has been found to show the best activity against the Y188L mutant of RT, with respect to the other pyrimidinones described in this paper (Table 1).

Starting from the crystallographic coordinates of RT, Tyr188 has been replaced with Leu in such a manner as the backbone atoms do not move and the remaining atoms of the side chain of the new residue assume a conformation comparable to that of the original amino acid.

Based on previous results showing no major main-chain movement in the Y188L mutant structure of the RT enzyme,[26] Y188L mutation is not expected to cause major structural changes in the RT structure. With the aim of calculating the possible orientation of the Leu188 side chain, a systematic conformational search was applied to the mutated amino acid residue. As a result, the side-chain of Leu188 could adopt a range of conformations, mainly due to the significant increase in the NNIBS volume in the RT Y188L mutant with respect to the wild type.[26]

Molecular docking and conformational searching of the ligand within the NNIBS have been performed to obtain the theoretical models of both the RT–**3b** and the RT–**3c** complex. As in other complexes between RT and NNRTI,

several hydrophobic residues of NNIBS are important in the binding of **3c** to RT (Fig. 2). In fact, the benzyl moiety of **3c** is accommodated within a hydrophobic pocket mainly defined by Val108, the mutated Leu188, and Phe227, with strong interactions between the phenyl ring of the ligand and the isopropyl group of the mutated Leu188. In addition, the aromatic side chain of Phe227 shows a T tilted orientation[27] with respect to the aromatic portion of the ligand, allowing for a profitable $\pi-\pi$ interaction. The isopropyl groups of both Val108 and Leu234 complete the hydrophobic pocket surrounding the benzyl moiety at the C-6 position. As also seen in all the complexes between RT and HEPT derivatives, the extended conformation of the long C-2 chain of **3c** causes the Pro236 loop to retain a conformation similar to that observed in the unliganded RT structure. The terminal C-2 hydroxy group makes a hydrogen bond with the carbonyl group of Leu234, while the sulphur atom is located at a distance of approximately 3.7 Å from the backbone NH group of Lys103. The complex is stabilized by a strong hydrogen bond between the NH group at position 3 of the pyrimidine ring and the carbonyl oxygen of Lys101 (1.8 Å distance).

While in the complexes with HEPT derivatives a water molecule, located in the NNIBS near a channel to the solvent, was found, the crystal data used in developing our model were not sufficiently resolved to permit the location of specific water molecules in the pocket.[22] As a consequence, we have performed two different simulations where a water molecule has or has not been included in the calculations. In the simulation with the explicit water molecule, we found a network of hydrogen bonds involving the water and Tyr181, Glu138 (in the p51 chain), Lys101, and, finally, the carbonyl group at 4-position of compound **3c**. In the complex without the water molecule, the hydroxy group of Tyr181 contacts by a hydrogen bond the Glu138 side chain. Actually, no substantial difference in the interaction mode has been found either including or excluding a water molecule. This result is not unexpected in the light of the reported high flexibility of NNIBS.

The most relevant structural difference in the complexes between RT and either **3c** or the corresponding 5-desmethyl derivative **3b** concerns the conformation of the Tyr181 side chain. In the RT–**3c** complex, the carbon atom of the C5-methyl group is located at a distance of 4.4 and 3.4 Å from the methylene group of both the Tyr181 and the mutated Leu188 side chains, respectively, allowing for profitable hydrophobic contacts. When the calculations were repeated using **3b** as the ligand instead of **3c**, the side chain of Tyr181 undergoes a conformational rearrangement leading to a structure almost undistinguishable from that found in the catalytically active p66 subunit of the unliganded enzyme. These findings are in good agreement with previous reports[22,25,28,29] showing that the group at the 5-position of HEPT derivatives is crucial in determining the conformational perturbation of the Tyr181 side chain. In particular, it has been highlighted that a 5-isopropyl substituent forces Tyr181 into a p51-like, catalytically inactive, conformation, thus resulting in a strong RT inhibitor. On the other hand, HEPT having a 5-methyl group produces slight conformational changes on Tyr181, and, accordingly, shows only a moderate inhibitory activity.

In this context, while compound **3c** induces a conformational rearrangement on Tyr181 similar to that caused by HEPT, in the RT-**3b** complex, the lack of the C5-substituent allows the Tyr181 side chain to retain a conformation very similar to that of the unbound p66 subunit.

In conclusion, we feel that the conformational rearrangement of the Tyr181 side chain, combined with some missing hydrophobic contacts in the complex RT–**3b** (between the 5-methyl group and the methylene portion of the Tyr181 and Leu188 side chains), might explain the four-fold decrease in the binding properties of **3b** with respect to **3c**.

3. Conclusions

5,6-Disubstituted 4(3*H*)-pyrimidinones **1**–**3** have been prepared in a profitable way through an SPS approach which favourably compares with the corresponding solution-phase synthesis, in that it avoids the laborious purification of the highly polar synthetic intermediates and provides the final compounds in good yield and purity. Pyrimidinones **1**–**3** can be regarded as molecular hybrids between DABO and HEPT derivatives, since they have at C2 position a tetramethylene side chain similar to that present in DABOs and S-DABOs, but bearing a polar (hydroxy or amino) group in the final position on the analogy of HEPT derivatives. The SPS approach here described proved indeed to be practicable also for the preparation of new DABOs and could provide a convenient access to small libraries of NNRTI based on a pyrimidinone structure, considering that many structurally diverse β-ketoesters are commercially available or can be easily synthesized. When evaluated as NNRTI in biological tests, compounds **1**–**3** have displayed an interesting anti-RT profile, generally characterized by modest or no activity against RT from wild type HIV accompanied by some selectivity towards RTs from mutant viruses. The reason for this selectivity has been explained through a molecular modeling study, based on molecular docking and a conformational search of inhibitors **3b** and **3c** within the NNIBS of Y188L RT. The comparison between the two complexes has highlighted the crucial role played by the C5 substituent of **3c** in causing conformational changes that lead to a catalytically inactive enzyme. Although the new compounds **1**–**3** cannot be considered as potential clinical candidates, they are nevertheless of interest as lead structures in the search of novel RT inhibitors.

4. Experimental

4.1. General methods

Unless otherwise stated, all reactions were carried out under an argon atmosphere. Reagents were obtained from commercial suppliers and used without further purifications. Merck silica gel 60 was used for both column chromatogaphy (70–230 mesh) and flash chromatography (230–400 mesh). Melting points are uncorrected. The NMR spectra were measured at 200 MHz. Chemical shifts are reported relative to $CDCl_3$ at δ 7.24 ppm and tetramethylsilane at δ 0.00 ppm. Infrared spectra were recorded on a

FT-IR spectrophotometer. EI and FAB low-resolution mass spectra were recorded with an electron beam of 70 eV. Elemental analyses (C, H, N) were performed 'in house'.

4.1.1. *N*,*N*′-Bis(*tert*-butoxycarbonyl)-*N*″-(4′-hydroxybutyl)guanidine (5). A solution of *N*,*N*′-bis(*tert*-butoxycarbonyl)-*S*-methylisothiourea (6.5 g, 22.4 mmol) in THF (50 mL) was added dropwise to a solution of 1-amino-4-butanol (5.0 g, 56.1 mmol) in THF (50 mL) and water (3.5 mL). After stirring at 50°C for 1 h, the solution was evaporated under reduced pressure and the residue was partitioned between $CHCl_3$ and water. The organic layer was washed with brine, dried (Na_2SO_4) and evaporated. Flash chromatography of the crude residue on silica gel (Et_2O) gave **5** (6.3 g, 85%) as a white solid: mp 124–125°C; IR ($CHCl_3$) 3330, 2976, 1723, 1623 cm^{-1}; ^1H NMR ($CDCl_3$) δ 1.46 (s, 18H), 1.54–1.77 (m, 4H), 2.11 (s, 4H), 3.36 (q, 2H, *J*=6.3 Hz), 3.62 (t, 2H, *J*=6.3 Hz), 8.36 (s, 1H), 11.44 (s, 1H). FABMS (TDEG-GLY) *m*/*z* 332 $(M+H)^+$. Anal. calcd for $C_{15}H_{29}N_3O_5$: C, 54.36; H, 8.82; N, 12.68. Found: C, 54.54; H, 8.79; N, 12.51.

4.1.2. Polymer-bound *N*,*N*′-Bis(*tert*-butoxycarbonyl)-guanidine 6. Resin **4** (2.20 g, 1.6 mmol) was suspended in dry CH_2Cl_2 (50 mL) and swollen for 10 min. A solution of **5** (1.99 g, 6.0 mmol) and Et_3N (836 μL, 6.0 mmol) in dry CH_2Cl_2 (10 mL) was added dropwise and the mixture was refluxed overnight. The resin was filtered, washed successively with water (3×10 mL), 50% aqueous EtOH (3×10 mL), $CHCl_3$ (2×10 mL) and Et_2O (5×10 mL), then dried in vacuo at 35°C for 3 h. IR (nujol) 1740, 1712, 1660, 1619 cm^{-1}.

4.1.3. Polymer-bound guanidinium salt 7. Resin **6** (2.67 g, 1.6 mmol) was suspended in dry dioxane (25 mL) and swollen for 10 min. Methanesulfonic acid (386 μL, 6.0 mmol) was added dropwise and the reaction mixture was refluxed overnight. The resin was filtered, washed with CH_2Cl_2 (5×20 mL), Et_2O (3×10 mL) and dried in vacuo at 115°C for 3 h to give 2.5 g (1.6 mmol) of solid supported guanidinium salt **7**. IR (nujol) 3300, 1740, 1619, 880 cm^{-1}.

4.2. Synthesis of 6-substituted 2-[1′-(4′-hydroxy)butyl]-amino-4(3*H*)-pyrimidinones (1a,b) and 6-substituted 2-amino-3-[1′-(4′-hydroxy)butyl]-4(3*H*)-pyrimidinones (9a,b): general procedure

Resin **7** (1 g, 0.64 mmol) was suspended in dry MeOH (15 mL) and swollen for 10 min. A solution of NaOMe, prepared by dissolving 72 mg (3.13 mmol) of Na in 8 mL of dry MeOH, was added dropwise followed by the appropriate β-keto ester **8a**, **b** (3.15 mmol). After stirring for 20 h under reflux, the mixture was cooled to rt and filtered. The resin was washed with methanol (3×10 mL), CH_2Cl_2 (3×10 mL) and Et_2O (3×20 mL). The combined filtrate and washings were concentrated in vacuo, neutralized with 1N HCl and extracted with $CHCl_3$ (5×10 mL). The organic layer was washed with brine, dried (Na_2SO_4) and evaporated. Flash chromatography on silica gel (10% MeOH in $CHCl_3$) of the solid residue afforded the title compounds.

4.2.1. 2-[1′-(4′-Hydroxy)butyl]amino-6-methyl-4(3*H*)-pyrimidinone (1a). 44.9 mg (36%). R_f 0.19. Mp 132–134°C; IR ($CHCl_3$) 3330, 2984, 1724, 1660 cm^{-1}; ^1H NMR ($CDCl_3$) δ 1.62–1.77 (m, 4H), 2.15 (s, 3H), 3.45 (t, 2H, *J*=5.9 Hz), 3.71 (t, 2H, *J*=5.8 Hz), 5.87 (s, 1H). ^{13}C NMR (CD_3OD, 55°C) δ 22.64, 26.85, 30.73, 41.70, 62.69, 101.64, 156.02, 168.94, 169.15. FABMS (TDEG-GLY) *m*/*z* 198 $(M+H)^+$. Anal. calcd for $C_9H_{15}N_3O_2$: C, 54.81; H, 7.67; N, 21.30. Found: C, 54.64; H, 7.76; N, 21.51.

4.2.2. 2-Amino-3-[1′-(4′-hydroxy)butyl]-6-methyl-4(3*H*)-pyrimidinone (9a). 14.2 mg (11%). R_f 0.21. Mp 164–166°C; IR ($CHCl_3$) 3330, 2984, 1724, 1514 cm^{-1}; ^1H NMR ($CDCl_3$) δ 1.68–1.83 (m, 4H), 2.20 (s, 3H), 3.75 (t, 2H, *J*=6.3 Hz), 4.095 (t, 2H, *J*=6.8 Hz), 5.89 (s, 1H), 6.60 (br s, 2H). ^{13}C NMR (CD_3OD) δ 21.94, 24.66, 30.16, 42.34, 62.45, 101.69, 155.94, 162.20, 163.87. FABMS (TDEG-GLY) *m*/*z* 198 $(M+H)^+$. Anal. calcd for $C_9H_{15}N_3O_2$: C, 54.81; H, 7.67; N, 21.30. Found: C, 54.99; H, 7.60; N, 21.15.

4.2.3. 6-Benzyl-2-[1′-(4′-hydroxy)butyl]amino-4(3*H*)-pyrimidinone (1b). 73.7 mg (42%). R_f 0.26. Mp 95–96°C; IR ($CHCl_3$) 3330, 2984, 1777, 1654 cm^{-1}; ^1H NMR ($CDCl_3$) δ 1.52–1.66 (m, 4H), 3.30 (m, 2H), 3.60–3.67 (s+m, 2H+2H), 5.49 (s, 1H), 7.23–7.37 (m, 5H). ^{13}C NMR (CD_3OD, 55°C) δ 26.92, 30.71, 41.70, 43.97, 62.60, 101.49, 127.62, 129.43, 130.25, 138.95, 155.91, 168.18, 168.80. FABMS (TDEG-GLY) *m*/*z* 274 $(M+H)^+$. Anal. calcd for $C_{15}H_{19}N_3O_2$: C, 65.91; H, 7.01; N, 15.37. Found: C, 66.13; H, 7.10; N, 15.20.

4.2.4. 2-Amino-6-benzyl-3-[1′-(4′-hydroxy)butyl]-4(3*H*)-pyrimidinone (9b). 21.3 mg (12%). R_f 0.29. Mp 196–198°C; IR ($CHCl_3$) 3330, 2984, 1724, 1514 cm^{-1}; ^1H NMR ($CDCl_3$) δ 1.68–1.83 (m, 4H), 3.68–3.82 (m, 2H+2H), 4.1 (t, 2H, *J*=6.8 Hz), 5.66 (s, 1H), 6.51 (br s, 2H), 7.35–7.60 (m, 5H). ^{13}C NMR (CD_3OD, 55°C) δ 24.74, 30.25, 42.20, 44.24, 62.48, 101.13, 127.65, 129.37, 130.31, 136.80, 156.96, 165.44, 169.06. FABMS (TDEG-GLY) *m*/*z* 274 $(M+H)^+$. Anal. calcd for $C_{15}H_{19}N_3O_2$: C, 65.91; H, 7.01; N, 15.37. Found: C, 66.19; H, 6.89; N, 15.19.

4.2.5. Polymer-bound 1,4-diaminobutane 11. Resin **10** (3.8 g, 4 mmol) was suspended in dry CH_2Cl_2 (100 mL) and swollen for 10 min. Dry pyridine (3.05 μL, 28.3 mmol) and 1,4-diaminobutane (2.49 g, 28.3 mmol) were added and the mixture was stirred at 25°C for 36 h. The resin was filtered and washed sequentially with CH_2Cl_2 (2×30 mL), MeOH (3×20 mL), CH_2Cl_2 (3×10 mL), and Et_2O (3×20 mL). The material was dried in vacuo at 25°C for 3 h to give 4 g (4 mmol) of solid supported 1,4-diaminobutane **16**. IR (nujol) 3300, 1712, 1601, 880 cm^{-1}.

4.2.6. Polymer-bound guanidine 12. Resin **11** (1.02 g, 1.02 mmol) was suspended in THF (13 mL) and water (250 μL) and swollen for 10 min. *N*,*N*′-Bis(*tert*-butoxycarbonyl)-*S*-methylisothiourea (2.7 g, 9.45 mmol) in THF (20 mL) was added and the mixture was stirred at 60°C for 60 h. The resin was filtered, washed with hot EtOH (3×20 mL), dioxane (3×10 mL), Et_2O (3×15 mL) and dried in vacuo at 35°C for 3 h. IR (nujol) 1712, 1660, 1619 cm^{-1}.

4.2.7. Polymer-bound guanidinium salt 13. Resin **12** (1.27 g, 1.02 mmol) was suspended in dry CH_2Cl_2 (12 mL) and swollen for 10 min. After cooling to 0°C, a 50% solution of TFA in dry CH_2Cl_2 (12 mL) was added dropwise and the suspension was stirred at 0°C for 3 h. The resin was filtered, washed with CH_2Cl_2 (5×10 mL), Et_2O (3×10 mL) and dried in vacuo at 35°C for 3 h. IR (nujol) 3300, 1712, 1660, 1619, 880 cm^{-1}.

4.3. Polymer-bound pyrimidinones 14/15b,c and pyrimidinones 16/17b,c: general procedure

Prepared following the procedure described for compounds **1** and **9** starting from resin **13**[19] (700 mg, ≅0.6 mmol) and β-keto esters **8b**, **c**. After stirring for 20 h at reflux temperature, the resin was filtered, washed and dried in vacuo at 25°C for 3 h to yield **14/15b**, **c**. IR (nujol) 1712, 1630, 1601 cm^{-1}.

The combined filtrate and washings were concentrated in vacuo, neutralized with 1N HCl and extracted with $CHCl_3$ (5×10 mL). The organic layer was washed with brine, dried (Na_2SO_4) and evaporated. Flash chromatography on silica gel (5% MeOH in $CHCl_3$) of the solid residue gave compounds **16** and **17**.

4.3.1. 6-Benzyl-2-[1′-(4′-methoxycarbonylamino)butyl]-amino-4(3*H*)-pyrimidinone (16b). 19.8 mg (10%). R_f 0.25. Mp 55–57°C; IR ($CHCl_3$) 3016, 1655, 1613 cm^{-1}; ^1H NMR ($CDCl_3$) δ 1.40–1.68 (m, 4H), 3.02–3.20 (m, 2H), 3.20–3.40 (m, 2H), 3.62 (s, 3H), 3.68 (s, 2H), 4.90–5.17 (m, 1H), 5.45 (s, 1H), 7.12–7.40 (m, 5H). ^{13}C NMR (CD_3OD) δ 25.24, 27.32, 41.78, 42.43, 44.61, 52.02, 101.08, 127.31, 129.12, 139.86, 156.43, 158.65, 162.08, 170.01. FABMS (TDEG-GLY) *m/z* 331 $(M+H)^+$. Anal. calcd for $C_{17}H_{22}N_4O_3$: C, 61.80; H, 6.71; N, 16.96. Found: C, 62.05; H, 6.81; N, 16.77.

4.3.2. 2-Amino-6-benzyl-3-[1′-(4′-methoxycarbonylamino)-butyl]-4(3*H*)-pyrimidinone (17b). 5.9 mg (3%). R_f 0.31. Mp 149–153°C; IR ($CHCl_3$) 3017, 1656, 1626 cm^{-1}; ^1H NMR ($CDCl_3$) δ 1.48–1.75 (m, 4H), 3.10–3.40 (m, 2H), 3.62 (s, 3H), 3.85–3.98 (m, 2H), 5.64 (s, 1H), 6.50 (br s, 2H), 7.10–7.32 (m, 5H). ^{13}C NMR (CD_3OD) δ 26.08, 28.31, 42.18, 43.95, 44.06, 53.37, 101.14, 127.64, 129.78, 139.01, 157.64, 161.49, 165.52, 170.17. FABMS (TDEG-GLY) *m/z* 331 $(M+H)^+$. Anal. calcd for $C_{17}H_{22}N_4O_3$: C, 61.80; H, 6.71; N, 16.96. Found: C, 61.99; H, 6.62; N, 16.75.

4.3.3. 6-Benzyl-2-[1′-(4′-methoxycarbonylamino)butyl]-amino-5-methyl-4(3*H*)-pyrimidinone (16c). 16.5 mg (8%). R_f 0.29. Mp 60–63°C; IR ($CHCl_3$) 3016, 1655, 1613 cm^{-1}; ^1H NMR ($CDCl_3$) δ 1.40–1.68 (s, 4H), 1.95 (s, 3H), 3.02–3.15 (m, 2H), 3.30–3.40 (m, 2H), 3.60 (s, 3H), 3.82 (s, 2H), 4.90–5.01 (m, 1H), 7.09–7.35 (m, 5H). ^{13}C NMR (CD_3OD) δ 11.32, 25.23, 27.18, 41.63, 42.05, 44.80, 51.53, 100.13, 127.09, 129.78, 139.67, 156.16, 157.41, 163.95, 171.12. FABMS (TDEG-GLY) *m/z* 345 $(M+H)^+$. Anal. calcd for $C_{18}H_{24}N_4O_3$: C, 62.77; H, 7.02; N, 16.27. Found: C, 62.55; H, 7.09; N, 16.39.

4.3.4. 2-Amino-6-benzyl-3-[1′-(4′-methoxycarbonylamino)-butyl]-5-methyl-4(3*H*)-pyrimidinone (17c). 4.1 mg (2%). R_f 0.33. Mp 142–145°C; IR ($CHCl_3$) 3017, 1656, 1626 cm^{-1}; ^1H NMR ($CDCl_3$) δ 1.52–1.75 (m, 4H), 1.98 (s, 3H), 3.14–3.32 (m, 2H), 3.60 (s, 3H), 3.72 (s, 2H), 3.81–3.98 (m, 2H), 6.51 (br s, 2H), 7.02–7.40 (m, 5H). ^{13}C NMR (CD_3OD) δ 11.48, 27.43, 28.76, 42.26, 43.07, 44.62, 52.86, 101.54, 127.33, 129.45, 139.61, 156.93, 165.06, 171.04. FABMS (TDEG-GLY) *m/z* 345 $(M+H)^+$. Anal. calcd for $C_{18}H_{24}N_4O_3$: C, 62.77; H, 7.02; N, 16.27. Found: C, 62.95; H, 6.93; N, 16.12.

4.4. Cleavage of pyrimidinones 2/18b, c: general procedure

Resins **14/15b** (0.52 mmol) or **14/15c** (0.55 mmol) were suspended in dry MeOH (40 mL) and swollen for 10 min. Pd–C (10%, 500 mg) and ammonium formate (198 mg, 3.15 mmol) were added and the mixture was refluxed for 20 min. The hot suspension was filtered on celite and washed with hot water (2×10 mL), hot MeOH (2×10 mL). Filtrate and washings were concentrated in vacuo to give a white solid which was extracted with hot MeOH (4×5 mL) and filtered. The methanolic extract was evaporated to leave a mixture of **2/18b**, **c**, which was separated by preparative TLC on silica gel (AcOEt/MeOH/NH_4OH 7/1.5/1.5) to afford the pure compounds.

4.4.1. 2-[1′-(4′-Amino)butyl]amino-6-benzyl-4(3*H*)-pyrimidinone (2b). 35.9 mg (22%). R_f 0.27. Mp 95–97°C; IR (nujol) 3030, 1656 and 1626 cm^{-1}; ^1H NMR (CD_3OD) δ 1.56–1.83 (m, 4H), 2.85–3.06 (m, 2H), 3.32–3.48 (m, 2H), 3.71 (s, 2H), 5.48 (s, 1H), 7.12–7.38 (m, 5H), 8.45 (br s, 1H). ^{13}C NMR (CD_3OD, 55°C) δ 25,71, 27,3, 40.31, 40.5, 40,79, 101.49, 127.59, 129.52, 129.66, 136,23, 154.33, 159.57, 169.8, 170.03. FABMS (TDEG-GLY) *m/z* 273 $(M+H)^+$. Anal. calcd for $C_{15}H_{20}N_4O$: C, 66.15; H, 7.40; N, 20.57. Found: C, 66.33; H, 7.51; N, 20.33.

4.4.2. 2-Amino-3-[1′-(4′-amino)butyl]-6-benzyl-4(3*H*)-pyrimidinone (18b). 4.9 mg (3%). R_f 0.38. Mp 125–128°C; IR (nujol) 3031, 1660 and 1630 cm^{-1}; ^1H NMR (CD_3OD) δ 1.2–1.4 (m, 4H), 3.28–3.38 (m, 2H), 3.64 (s, 2H), 3.91–4.04 (m, 2H), 5.57 (s, 1H), 7,10–7.45 (m, 5H), 8.45 (br s, 1H). ^{13}C NMR (CD_3OD, 55°C) δ 24.81, 26.94, 40.35, 41.82, 44.95, 101.72, 127.57, 129.51, 129.65, 136.23, 155.83, 170.15. FABMS (TDEG-GLY) *m/z* 273 $(M+H)^+$. Anal. calcd for $C_{15}H_{20}N_4O$: C, 66.15; H, 7.40; N, 20.57. Found: C, 66.39; H, 7.54; N, 20.30.

4.4.3. 2-[1′-(4′-Amino)butyl]amino-6-benzyl-5-methyl-4(3*H*)-pyrimidinone (2c). 44.6 mg (26%). R_f 0.29. Mp 110–113°C; IR (nujol) 3025, 1658 and 1627 cm^{-1}; ^1H NMR (CD_3OD) δ 1.56–1.83 (m, 4H), 1.88 (s, 3H), 2.85–3.06 (m, 2H), 3.32–3.48 (m, 2H), 3.75 (s, 2H), 7.02–7.31 (m, 5H), 8.45 (br s, 1H). ^{13}C NMR (CD_3OD, 55°C) δ 10.64, 25,71, 27,3, 40.31, 40.5, 40,79, 127.59, 129.52, 129.66, 136,23, 154.33, 159.57, 170.23, 171.35. FABMS (TDEG-GLY) *m/z* 287 $(M+H)^+$. Anal. calcd for $C_{16}H_{22}N_4O$: C, 67.11; H, 7.74; N, 19.56. Found: C, 66.89; H, 7.69; N, 19.70.

4.4.4. 2-Amino-3-[1′-(4′-amino)butyl]-6-benzyl-5-methyl-4(3*H*)-pyrimidinone (18c). 6.9 mg (4%). R_f 0.42. Mp 131–135°C; IR (nujol) 3030, 1660 and 1625 cm^{-1}; ^1H NMR (CD_3OD) δ 1.2–1.4 (m, 4H), 1.88 (s, 3H), 3.28–3.38 (m,

2H), 3.64 (s, 2H), 3.91–4.04 (m, 2H), 7,10–7.45 (m, 5H), 8.45 (br s, 1H). ^{13}C NMR (CD_3OD, 55°C) δ 11.43, 24.78, 26.85, 42.11, 44.81, 101.49, 127.59, 129.52, 129.63, 139.36, 156.83, 164.27, 169.16. FABMS (TDEG-GLY) *m/z* 287 $(M+H)^+$. Anal. calcd for $C_{16}H_{22}N_4O$: C, 67.11; H, 7.74; N, 19.56. Found: C, 67.33; H, 7.66; N, 19.38.

4.4.5. Polymer-bound pyrimidinones 23a–c. Treatment of resin **10** (950 mg, 1.008 mmol) with 4-chlorobutanol in the presence of pyridine, as described for the preparation of **11**, gave resin **19**, which in turn was refluxed for 72 h in EtOH (20 mL) in the presence of thiourea (240 mg, 3.15 mmol). The resin was then filtered and washed with hot ethanol (3×30 mL), dioxane (2×20 mL), and Et_2O (3×20 mL) and finally dried in vacuo at 35°C for 3 h to yield 1.099 g (1.008 mmol) of **20**. IR (nujol) 1740, 1637, 1601 cm^{-1}.

4.5. Polymer-bound pyrimidinones 3a–c: general procedure

Resin **20** (142 mg, 0.13 mmol) was swollen for 15 min in 50% aqueous MeOH (30 mL). The appropriate β-keto ester **8a–c** (2.6 mmol) and $Ca(OH)_2$ (24 mg, 0.32 mmol) were added and the mixture was stirred at rt for 72 h. The resin was filtered, washed sequentially with hot water (5×10 mL), 50% aqueous EtOH (3×10 mL), EtOH (3×15 mL), CH_2Cl_2 (3×15 mL), Et_2O (3×15 mL) and finally dried in vacuo at 35°C for 3 h to afford the title compounds. IR (nujol) 1740, 1630, 1601 cm^{-1}.

4.6. Cleavage of pyrimidinones 3a–c: general procedure

Polymer-bound pyrimidinones **23a–c** (0.13 mmol) were suspended in dry CH_2Cl_2 (8 mL) and swollen for 10 min. TFA (320 μL) was then added and the suspension was stirred at rt for 48 h. The resin was filtered, washed with MeOH/$CHCl_3$ 1/1 (3×10 mL), $CHCl_3$ (2×10 mL), CH_2Cl_2 (2×10 mL) and Et_2O (3×10 mL). The combined filtrate and washings were concentrated in vacuo to give **3a–c** as off-white crystals.

4.6.1. 2-[1′-(4′-Hydroxy)butyl]thio-6-methyl-4(3*H*)-pyrimidinone (3a). 21.6 mg (77%). Mp 164–166°C; IR ($CHCl_3$) 3368, 3015, 1641 cm^{-1}; ^{1}H NMR (CD_3OD) δ 0.8–0.9 (m, 2H), 1.20–1.35 (m, 4H), 1.49–1.65 (m, 4H), 2.23 (s, 3H), 2.52–2.68 (m, 2H), 3.48–3.60 (m, 2H), 3.65 (s, 1H), 5.62 (s, 1H). ^{13}C NMR (CD_3OD) δ 22.74, 30.71, 31.16, 34.12, 62.70, 101.49, 159.02, 168.12, 169.77. FABMS (TDEG-GLY) *m/z* 215 $(M+H)^+$. Anal. calcd for $C_9H_{14}N_2O_2S$: C, 50.45; H, 6.59; N, 13.07. Found: C, 50.63; H, 6.49; N, 13.20.

4.6.2. 2-[1′-(4′-Hydroxy)butyl]thio-6-benzyl-4(3*H*)-pyrimidinone (3b). 31.4 mg (83 %). Mp 196–198°C; IR ($CHCl_3$) 3365, 3013, 1640 cm^{-1}; ^{1}H NMR ($CDCl_3$) δ 1.15–1.40 (m, 4H), 1.49–1.65 (m, 4H), 3.40–3.55 (m, 2H), 3.69–3.79 (m, 2H), 5.71 (s, 1H), 7.24–7.38 (m, 5H). ^{13}C NMR (CD_3OD) δ 30.01, 31.84, 34.58, 43.67, 62.03, 101.81, 127.98, 129.01, 139.46, 159.44, 168.13, 169.69. FABMS (TDEG-GLY) *m/z* 291 $(M+H)^+$. Anal. calcd for $C_{15}H_{18}N_2O_2S$: C, 62.04; H, 6.25; N, 9.65. Found: C, 61.79; H, 6.33; N, 9.45.

4.6.3. 2-[1′-(4′-Hydroxy)butyl]thio-6-benzyl-5-methyl-4(3*H*)-pyrimidinone (3c). 32.6 mg (82%). Mp. 186–188°C; IR ($CHCl_3$) 3370, 3016, 1640 cm^{-1}; ^{1}H NMR ($CDCl_3$) δ 1.58 (s, 4H), 2.01 (s, 2H), 2.03 (s, 3H), 3.85 (s, 2H), 7.12–7.35 (m, 5H). ^{13}C NMR (CD_3OD) δ 11.51, 30.38, 31.49, 34.56, 44.08, 62, 23, 100.84, 127.14, 129.06, 139.78, 159.81, 168.21, 169.70. FABMS (TDEG-GLY) *m/z* 305 $(M+H)^+$. Anal. calcd for $C_{16}H_{20}N_2O_2S$: C, 63.13; H, 6.62; N, 9.20. Found: C, 62.91; H, 6.73; N, 9.02.

4.7. Computational methods

All calculations and graphical manipulations were performed on a Silicon Graphics Indy workstation using the software package MacroModel/BatchMin[30] equipped with the AMBER* united-atom force field.[31,32] The enzyme model used in this study was derived from the structure of the complex between HIV-1 RT and 1-(2-hydroxyethoxymethyl)-6-phenylthiothymine (HEPT), refined at 3.0 Å resolution (code 1rti in the Brookhaven Protein Data Bank).

To create initial coordinates for the docking studies, all water molecules of the crystal structure were removed and excluded from the calculations. Moreover, Tyr188 was replaced by a Leu residue.

The inhibitor (HEPT) in the X-ray crystal structure was used to guide the building of the complex between **3c** and RT providing a good template to locate compound **3c** into the NNIBS. The starting model was built by superimposition of the C5–C4–N3 sequence of both **3c** and HEPT (in its complex with RT).

Hydrogens and lone pairs were attached to heteroatoms and sulphur atoms, respectively, in their idealized positions to the amino acid residues included in the below described subset and shells.

The complex generated was then submitted to a systematic conformational search with Systematic Pseudo Monte Carlo (SPMC) method involving the rotatable bond of the ligand, Leu188 side chain, and Tyr181 side chain. The resolution for torsional alterations was set to a range of values between 3 and 24 (corresponding to 120 and 15 degrees rotations, respectively) for all the rotatable bonds.

MOLS command was used to allow for both the translation and rotation of the ligand within the NNIBS.

The GB/SA solvation method (water as the solvent) was applied to all the calculations.

The least square superimposition routine was selected (COMP command) to compare each new complex with all conformers previously found in order to eliminate duplicate minima. In particular, structures were considered to be the same unless one or more pairs of equivalent atoms were found to be separated by more than 0.25 Å.

Because of the large number of atoms in the model, to correctly optimize the complex of the inhibitor and RT, the following constraints had to be imposed: (a) a subset, centered on the inhibitor and comprising only the ligand and

a shell of residues surrounding the binding site of the enzyme within a radius of 10 Å from the ligand, was created and subjected to energy minimization. The inhibitor and all amino acid side chains of the shell were unconstrained during energy minimization to allow for reorientation and hence proper hydrogen-bonding geometries and vdW contacts. (b) In order to prevent their distortion during the conformational search and subsequent energy minimization, three shells of atoms external to the first subset were constrained using distance dependent restraining potentials of 100, 200, and 500 kJ $Å^{-2}$, respectively.

Energy minimization of the complexes was performed using the Polak–Ribière conjugate gradient method until the derivative convergence was 0.01 kcal $Å^{-1}mol^{-1}$. The default non-bonded cutoff protocol employed by the program was modified. Thus, a vdW cutoff of 12.0 Å, an electrostatic cutoff of 20 Å, and a hydrogen bonding cutoff of 2.5 Å were utilized for all calculations.

Acknowledgements

We thank Dr G. Delle Monache, CNR, Rome, Italy for measuring the ^{13}C NMR spectra. Financial support of this research by Istituto Superiore di Sanità, Roma, Italy (II Programma Nazionale di Ricerca sull'AIDS-1998, grant no. 40B.69 and III Programma Nazionale di Ricerca sull'AIDS-1999, grant no. 40C.65) as well as by the University of Siena (PAR 1999) is gratefully acknowledged. M. B. wishes to thank the Merck Research Laboratories for the 2001 Academic Development Program (ADP) Chemistry Award.

References

1. For part 1, see: Manetti, F.; Corelli, F.; Mongelli, N.; Lombardi Borgia, A.; Botta, M. *J. Comput-Aided Mol. Des.* **2000**, *14*, 355–368.
2. Guillier, F.; Orain, D.; Bradley, M. *Chem. Rev.* **2000**, *100*, 2091–2157.
3. Obrecht, D.; Villalgordo, J. M. *Solid-Supported Combinatorial and Parallel Synthesis of Small-Molecular-Weight Compound Libraries*; *Tetrahedron Organic Chemistry Series*, Vol. 17; Elsevier: Oxford, 1998.
4. (a) Brown, D. J. *The Chemistry of Heterocyclic Compounds*; Taylor, E. C., Weissberger, A., Eds.; Wiley: New York, 1994; Vol. 52, pp. 371–377. (b) Vedernikova, I. V.; Haemers, A.; Ryabukhin, Y. I. *J. Heterocycl. Chem.* **1999**, *36*, 97–104 and references cited therein. (c) Obrecht, D.; Abrecht, C.; Grieder, A.; Villalgordo, J. M. *Helv. Chim. Acta* **1997**, *80*, 65–72.
5. Botta, M.; Occhionero, F.; Nicoletti, R.; Mastromarino, R.; Conti, C.; Magrini, M.; Saladino, R. *Bioorg. Med Chem.* **1999**, *7*, 1925–1931.
6. Kim, D. K.; Gam, J.; Kim, Y. W.; Lim, J.; Kim, H. T.; Kim, K. H. *J. Med. Chem.* **1997**, *40*, 2363–2373.
7. Pontikis, R.; Benhida, R.; Aubertin, A. M.; Grierson, D. S.; Monneret, C. *J. Med. Chem.* **1997**, *40*, 1845–1854.
8. (a) Balzarini, J.; Karlsson, A.; De Clercq, E. *Mol. Pharmacol.* **1993**, *44*, 694–701. (b) Baba, M.; Tanaka, H.; Miyasaka, T.; Yuasa, S.; Ubasawa, M.; Walker, R. T.; De Clercq, E. *Nucleosides Nucleotides* **1995**, *14*, 575–584.
9. (a) Mai, A.; Artico, M.; Sbardella, G.; Massa, S.; Novellino, E.; Greco, G.; Loi, A. G.; Tramontano, E.; Marongiu, M. E.; La Colla, P. *J. Med. Chem.* **1999**, *42*, 619–627. (b) Mai, A.; Artico, M.; Sbardella, G.; Quartarone, S.; Massa, S.; Loi, A. G.; De Montis, A.; Scintu, F.; Putzolu, M.; La Colla, P. *J. Med. Chem.* **1997**, *40*, 1447–1454.
10. For recent reviews on anti-HIV agents, see: (a) Pedersen, O. S.; Pedersen, E. B. *Synthesis* **2000**, 479–495. (b) Pedersen, O. S.; Pedersen, E. B. *Antiviral Chem. Chemother.* **1999**, *10*, 285–314. (c) De Clercq, E. *Collect. Czech. Chem. Commun.* **1998**, *63*, 449–479. (d) Artico, M. *Il Farmaco* **1996**, *51*, 305–331.
11. (a) Ref. 1 (b) Krikorian, D.; Parushev, S.; Tarpanov, V.; Mechkarova, P.; Mikhova, B.; Botta, M.; Corelli, F.; Maga, G.; Spadari, S. *Med. Chem. Res.* **1997**, *7*, 546–556. (c) Botta, M.; Saladino, R.; Anzini, M.; Corelli, F. *Nucleosides Nucleotides* **1994**, *8*, 1769–1777.
12. For a preliminary communication, see: Nizi, E.; Botta, M.; Corelli, F.; Manetti, F.; Messina, F.; Maga, G. *Tetrahedron Lett.* **1998**, *39*, 3307–3310.
13. Botta, M.; Saladino, R.; Occhionero, F.; Nicoletti, R. *Trends Org. Chem.* **1995**, *5*, 57–81.
14. Botta, M.; Occhionero, F.; Saladino, R.; Crestini, C.; Nicoletti, R. *Tetrahedron Lett.* **1997**, *38*, 8249–8252.
15. Aryes, J. T.; Mann, C. K. *Polymer Lett. (Part B)* **1965**, *3*, 505–508.
16. Delle Monache, G.; Botta, B.; Delle Monache, F.; Espinal, R.; De Bonnevaux, S. C.; De Luca, C.; Botta, M.; Corelli, F.; Carmignani, M. *J. Med. Chem.* **1993**, *36*, 2956–2963.
17. No attempt was made to establish whether the cleavage reaction follows or precedes the condensation of the guanidine moiety with ketoesters.
18. Arnold, L. D.; Vederas, J. C. *J. Am. Chem. Soc.* **1989**, *111*, 3973–3976.
19. Resin **13** was subjected to hydrogenolysis (HCO_2NH_4/Pd–C) to give 4-aminobutylguanidine (agmatine), identical with an authentic sample available in our laboratory.[20] Based on the recovered agmatine, the loading of **13** was calculated to be ≅0.8 mmol/g.
20. Delle Monache, G.; Volpe, A. R.; Delle Monache, F.; Vitali, A.; Botta, B.; Espinal, R.; De Bonnevaux, S. C.; De Luca, C.; Botta, M.; Corelli, F.; Carmignani, F. *Bioorg. Med. Chem. Lett.* **1999**, *9*, 3249–3254.
21. (a) Botta, M.; Cavalieri, M.; Ceci, D.; De Angelis, F.; Finizia, G.; Nicoletti, R. *Tetrahedron* **1984**, *17*, 3313–3320. (b) Botta, M.; Artico, M.; Massa, S.; Gambacorta, A.; Marongiu, M. E.; Pani, A.; La Colla, P. *Eur. J. Med. Chem., Chim. Thér.* **1992**, *27*, 251–257. (c) Artico, M.; Massa, S.; Mai, A.; Marongiu, M. E.; Piras, G.; Tramontano, E.; La Colla, P. *Antivir. Chem. Chemother.* **1993**, *4*, 361–368.
22. Hopkins, A. L.; Ren, J.; Esnouf, R. M.; Willcox, B. E.; Jones, E. Y.; Ross, C.; Miyasaka, T.; Walker, R. T.; Tanaka, H.; Stammers, D. K.; Stuart, D. I. *J. Med. Chem.* **1996**, *39*, 1589–1600.
23. Mai, A.; Artico, M.; Sbardella, G.; Massa, S.; Loi, A. G.; Tramontano, E.; Scano, P.; La Colla, P. *J. Med. Chem.* **1995**, *38*, 3258–3263.
24. Arnold, E.; Das, K.; Ding, J.; Yadav, P. N. S.; Hsiou, Y.; Boyer, P. L.; Hughes, S. H. *Drug Des. Discov.* **1996**, *13*, 29–47.
25. Ren, J.; Esnouf, R.; Garman, E.; Somers, D.; Ross, C.; Kirby, I.; Keeling, J.; Darby, G.; Jones, Y.; Stuart, D.; Stammers, D. *Nature Struct. Biol.* **1995**, *2*, 293–302.
26. Hsiou, Y.; Das, K.; Ding, J.; Clark Jr, A. D.; Kleim, J. P.;

Rosner, M.; Winkler, I.; Riess, G.; Hughes, S. H.; Arnold, E. *J. Mol. Biol.* **1998**, *284*, 313–323.
27. Jorgensen, W. L.; Severance, D. L. *J. Am. Chem. Soc.* **1990**, *112*, 4768–4774.
28. Esnouf, R.; Ren, J.; Ross, C.; Jones, Y.; Stammers, D.; Stuart, D. *Nature Struct. Biol.* **1995**, *2*, 303–308.
29. Ren, J.; Esnouf, R.; Hopkins, A.; Ross, C.; Jones, Y.; Stammers, D.; Stuart, D. *Structure* **1995**, *3*, 915–926.
30. Mohamadi, F.; Richards, N. G. J.; Guida, W. C.; Liskamp, R.; Lipton, M.; Caufield, C.; Chang, G.; Hendrickson, T.; Still, W. C. *J. Comput. Chem.* **1990**, *11*, 440–458.
31. Weiner, S. J.; Kollman, P. A.; Case, D. A.; Singh, U. C.; Ghio, C.; Alagona, G.; Profeta, S.; Weiner, P. *J. Am. Chem. Soc.* **1984**, *106*, 765–784.
32. Weiner, S. J.; Kollman, P. A.; Nguyen, D. T.; Case, D. A. *J. Comput. Chem.* **1986**, *7*, 230–252.